



## A Physical Approach for SAR Speckle Simulation: First Results

Gerardo Di Martino\*, Antonio Iodice, Daniele Riccio and Giuseppe Ruello

University of Naples Federico II, Via Claudio 21, 80125, Napoli, Italy

\*Corresponding author, e-mail address: gerardo.dimartino@unina.it

### Abstract

In this paper a SAR simulator able to provide images presenting appropriate speckle statistics is introduced. The simulator is able to generate both Exponential (*fully developed* speckle) and K-distributed speckle statistics, according to surface and radar parameters. It is based on sound physical models for the evaluation of the number of equivalent scatterers per resolution cell. The proposed simulator requires as inputs the radar, orbital and surface parameters. The statistics relevant to each single equivalent scatterer are then effectively generated as a 2-D scale mixture of Gaussians and the global statistics of the return from each resolution cell are obtained as the coherent sum of all the scatterers contributions. The rationale of the proposed simulation framework is detailed and meaningful results regarding the analysis of the first simulated images are discussed.

**Keywords:** Synthetic Aperture Radar, Speckle, SAR simulation.

### Introduction

Synthetic Aperture Radar (SAR) single look images are affected by the presence of speckle, due to the occurrence of interference phenomena between different returns coming from the same resolution cell. In practical cases the deterministic knowledge of the structure of the observed surface at wavelength scale is not available, and a statistical description of the SAR images must be introduced: the received signal is described as the coherent sum of the returns coming from independent scatterers randomly distributed in the resolution cell [Jakeman and Pusey, 1976, 1978; Goodman, 1976, 2008; Oliver, 1984]. A reliable statistical characterization of the speckle is of key importance for a huge set of applications, e.g. model-based despeckling [Di Martino et al., 2012a, 2013a] and segmentation [Collins and Allan, 2009]. Therefore, a key parameter for the statistical characterization of the speckle is the number of independent scatterers per resolution cell,  $N$ .

Under the hypothesis that  $N \gg 1$ , the central limit theorem can be applied giving rise to a Gaussian complex circular process, with an Exponential distributed intensity and a phase uniformly distributed in  $(0, 2\pi)$ . In this case the speckle is defined to be *fully developed* [Goodman, 1976]. For low resolution SAR sensors, whose resolution cell area is of the

order of tenth of square meters, the Exponential model well matches with actual data. However, with the increasing availability of space-borne very high resolution SAR data, for which the hypothesis of a resolution cell size much larger than the wavelength cannot be always assumed, in many actual cases the statistics of SAR images can depart from those predicted by the Rayleigh model. In the past decades, in many actual situations the K-distribution - originally introduced for the analysis of sea clutter [Jakeman and Pusey, 1976] - has been successfully used to model the statistical behaviour of SAR images, as a function of the number of scatterers per resolution cell [Jakeman and Pusey, 1976, 1978; Oliver, 1984; Goodman, 2008].

In [Di Martino et al., 2010] preliminary results regarding the statistical characterization of very high resolution SAR images were presented. Afterwards, in [Di Martino et al., 2012, 2013] the authors introduced a theoretical framework aimed at providing a physical definition for the concept of equivalent “scatterer”, thus allowing an analytical evaluation of the number of equivalent scatterers present in resolution cells with fixed size. Apart from the sea surface, natural bare – or little vegetated – soil is of interest: this type of surfaces is effectively modelled through fractals and, more specifically, an fBm model for the observed surface is there assumed [Mandelbrot, 1983; Feder, 1988; Falconer, 1989; Franceschetti and Riccio, 2007]. The number of scatterers  $N$  is a function of both the roughness of the surface, which is described through its fractal parameters [Dierking, 1999; Shepard et al., 2001; Franceschetti and Riccio, 2007], and of the sensor parameters, such as the electromagnetic wavelength and resolution cell area. The ability to compute the number of equivalent scatterers per resolution cell for a given sensor and for a surface presenting prescribed fractal parameters can be exploited to introduce new techniques for the simulation of speckle in SAR images.

The interpretation of SAR data is often difficult, due to the fact that SAR images are related by non-linear relations with the scene parameters. Therefore, it is crucial to have efficient tools able to predict the SAR data behaviour as a function of the scene parameters. As a matter of fact, the use of a SAR simulator can provide value-added information for SAR data interpretation and a support for SAR processing techniques (e.g., image despeckling [Di Martino et al., 2012a, 2013a], segmentation [Lee and Jurkevich, 1989; Collins and Allan, 2009], change detection [Di Martino et al., 2007], sea target (and extended target) detection [Watts et al., 1990; Tello et al., 2007]).

In this paper a SAR simulator able to provide images presenting the appropriate speckle statistics is introduced. It requires as inputs the radar and surface parameters and - based on the model presented in [Di Martino et al., 2013] - it is able to compute the number of scatterers per resolution cell,  $N$ . Then, the statistics relevant to each single scatterer in the resolution cell are effectively synthesized [Eltoft, 2006] and the global statistics of the return from the resolution cell are obtained as the coherent sum of the individual scatterers contributions. The presented simulator is largely based on the SAR raw signal simulator (SARAS) (introduced in [Franceschetti et al., 1992] and positively tested in [Franceschetti et al., 1994]), which is able to provide images presenting fully developed speckle statistics in accordance with the acquisition parameters of the selected SAR sensor [Tomiyasu, 1983; Raney and Wessels, 1988]. The approach adopted in the present work updates the ability of the SARAS simulator to the generation of K distributed speckle, with  $N$  depending on the scene and sensor parameters.

The paper is organized as follows. In Section 2 the considered stochastic model of speckle is introduced. In Section 3 we summarize the basic concepts of the model introduced by the authors in [Di Martino et al., 2013] for the evaluation of the number of scatterers per resolution cell. The proposed simulation framework and the obtained simulated images are presented in Section 4 and 5, respectively. Finally, Section 6 bears some concluding remarks.

### Speckle statistical model

The return from each SAR resolution cell can be modelled as the coherent sum of  $N$  electromagnetic returns [Goodman, 1976; Jakeman and Pusey, 1976]:

$$E = Ve^{j\varphi} = \sum_{i=1}^N V_i e^{j\varphi_i} \quad [1]$$

where  $V_i e^{j\varphi_i}$  is the contribution due to the  $i$ -th scatterer. Hence, the field  $E$  is a function of the number of scatterers per resolution cell,  $N$ . According to this value, the speckle can be Exponentially or K-distributed: in particular, the Exponential distribution can be regarded as a particular case of the K-distribution for  $N \gg 1$  [Jakeman and Pusey, 1976]. If the hypothesis of a large number of independent scatterers per resolution cell does not hold, we must face the problem of studying the coherent sum of a finite number of terms [Goodman, 2008]. In order to obtain a closed form pdf for the return intensity, we can make the following assumptions [Jakeman and Pusey, 1976]:

- 1) the amplitudes  $V_i$  and the phases  $\varphi_i$  are statistically independent from each other and from  $V_j$  and  $\varphi_j$  if  $i \neq j$ ;
- 2) the  $V_i$  are K-distributed, i.e.:

$$p(V_i) = \frac{2b}{\Gamma(1+\nu)} \left( \frac{bV_i}{2} \right)^{\nu+1} K_\nu(bV_i) \quad [2]$$

where  $\nu > -1$  and  $b$  are parameters depending on the scene,  $K_\nu(\bullet)$  is the second kind modified Bessel function of order  $\nu$  and  $\Gamma(\bullet)$  is the Euler Gamma function;

- 3) the  $\varphi_i$  are uniformly distributed in  $[0, 2\pi]$ .

Under these hypotheses, the return intensity  $w = |E|^2$  presents a pdf that can be expressed as [Jakeman and Pusey, 1976]:

$$p_N(w) = \frac{b/\sqrt{w}}{\Gamma(M)} \left( \frac{b\sqrt{w}}{2} \right)^M K_{M-1}(b\sqrt{w}) \quad [3]$$

where the parameter  $M$  is related to the number of scatterers per resolution cell by the relation  $M = N(1+\nu)$ . The normalized moments associated to the distribution in [3] are given by

$$\frac{\langle w^n \rangle}{\langle w \rangle^n} = \left( \frac{2}{b} \right)^{2n} \frac{n! \Gamma(n+M)}{\Gamma(M)} \quad [4]$$

and the mean of the distribution is

$$\langle w \rangle = \left( \frac{2}{b} \right)^2 M \quad [5]$$

It can be shown that for  $M \gg 1$ , the distribution [3] reduces to a negative exponential function, i.e. the K-distribution model reduces to the Exponential one [Jakeman and Pusey, 1976]. It is well known that for the latter distribution the  $n$ -th normalized moment is equal to  $n!$ . The plots of the Exponential and K pdf (for  $N=\{1,2,5\}$ ) with unitary mean are reported in Figure 1.

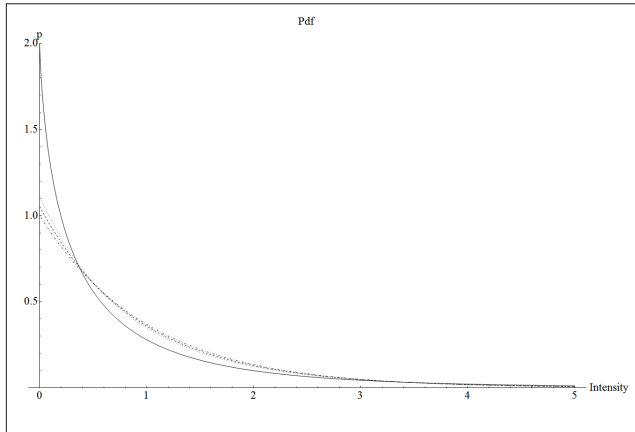


**Figure 1 - Graphs of the speckle pdf:  $N=1$  (full line),  $N=2$  (dotted line),  $N=5$  (dashed line), Exponential (dash-dotted line).**

## Models used for simulation

The above described models are purely statistical ones: they do not provide a definition of the scatterers, and they cannot directly relate the number of scatterers to the physical parameters characterizing the observed surface. As a matter of fact, only the Maxwell equations are able to provide a physical counterpart of the concept of scatterer, as well as a deeper understanding of the speckle phenomenon. In previous papers the authors introduced a model relating the purely mathematical concept of scatterers to physical properties of the observed surface via scattering models [Di Martino et al., 2012, 2013]. In this section we summarize these previous results, which stand as the basis of the present work.

### Surface model

The choice of an adequate model for the observed surface is crucial for scattering evaluation purposes. In literature, the most widespread models describe the rough surface shape as a

stationary Gaussian process [Beckman and Spizzichino, 1963]. However, in the last decades it was demonstrated that fractal models are the most accurate ones for the description of natural surfaces [Mandelbrot, 1983; Feder, 1988; Falconer, 1989; Dierking, 1999; Shepard et al., 2001; Franceschetti and Riccio, 2007]. In particular, only fractal models are able to take into account the scaling properties typical of natural surfaces [Falconer, 1989; Dierking, 1999; Shepard et al., 2001].

One of the most widespread fractal surface models is the fractional Brownian motion (fBm) model [Franceschetti and Riccio, 2007]. The fBm is an everywhere continuous, nowhere differentiable process, described in terms of its increment pdf. A stochastic process  $z(x,y)$  is an fBm surface if, for every  $x, x', y, y'$  it satisfies the following relation:

$$\Pr \left\{ z(x, y) - z(x', y') < \xi \right\} = \frac{1}{\sqrt{2\pi T^{1-H} \tau^H}} \int_{-\infty}^{\xi} \exp\left(-\frac{\xi^2}{2T^{2-2H} \tau^{2H}}\right) d\xi \quad [6]$$

where, as in the previous case,  $\tau$  is the distance between the points  $(x,y)$  and  $(x',y')$  and the two parameters that control the fBm behaviour are:

- $H$ : the *Hurst coefficient* ( $0 < H < 1$ ), related to the fractal dimension  $D$  by means of the relationship  $D=3-H$ ;
- $T$  [m]: the *topothesy*, i.e. the distance over which chords joining points on the surface have a surface-slope mean-square deviation equal to unity.

Note that in this case the shape of the structure function derives directly from the incremental process characterization [6], hence, with respect to classical models, no arbitrary choice of the correlation function must be performed. In particular, the fBm structure function is

$$Q(\tau) \triangleq \langle |z(x, y) - z(x', y')|^2 \rangle = T^{2-2H} \tau^{2H} \quad [7]$$

Note that the structure function in [7] is an increasing function of the distance  $\tau$ .

**Electromagnetic model for the evaluation of  $N$**

The SAR image is the superposition of the reflectivity function  $\gamma(\bullet)$ , weighted by the overall (i.e., including the focusing) system unit response  $g(\bullet)$ :

$$i(x_0, y_0) = \iint \gamma(x, y) g(x_0 - x, y_0 - y) dx dy \quad [8]$$

The reflectivity function  $\gamma(x,y)$  can be expressed as the product of a polarization factor  $S$ , depending on surface electric permittivity, incidence angle and polarizations, and a (two-way) propagation factor  $e^{-j2kR} e^{j2\mathbf{k}\cdot\mathbf{r}}$ , accounting for phase contributions coming from the points of the resolution cell located in position  $\mathbf{r} = \hat{x}x + \hat{y}y + \hat{z}z(x,y)$ . Here,  $\mathbf{k} = k_x \hat{x} + k_y \hat{y} + k_z \hat{z}$  is the electromagnetic propagation vector, so that  $\|\mathbf{k}\| = k = 2\pi / \lambda$  ( $\lambda$  is the transmitted signal wavelength), and  $R$  is the distance of the sensor from the origin

of the reference system. The function  $g(\bullet)$  is assumed to be negligible outside an area  $A$  centred around  $(x_0, y_0)$ , here defined as the “resolution cell”, while  $S$  can be reasonably considered constant within each resolution cell. Therefore, the value assumed by the SAR image in the centre  $(x_0, y_0)$  of a generic resolution cell can be evaluated according to the following expression:

$$i(x_0, y_0) = S e^{-j2kR} \iint e^{j2k_x x} e^{j2k_y y} e^{j2k_z z(x,y)} g(x_0 - x, y_0 - y) dx dy \quad [9]$$

In order to attain a physical definition of the scatterers allowing the evaluation of the pdf in [3], we can subdivide the resolution cell into smaller domains, each representing a single “equivalent scatterer”, in such a way that returns pertaining to a single domain are correlated, whereas returns from different domains are uncorrelated. To obtain a proper evaluation of the equivalent scatterer size, we define the scatterer radius  $\tau_M$  as the distance between the two generic surface points  $(x, y)$  and  $(x', y')$  such that the correlation between returns from the two points, i.e.,

$$\langle e^{j2k_z z(x,y)} e^{-j2k_z z(x',y')} \rangle = \langle e^{-j2k_z (z(x',y') - z(x,y))} \rangle = e^{-\frac{(2k_z)^2}{2} Q(\tau)} \quad [10]$$

falls below a given threshold, say  $e^{-t}$  (with  $t$  of the order of unity). Substituting the structure function [7], we obtain the following size for the equivalent scatterers radius:

$$\tau_M = \left( \frac{\sqrt{t}}{\sqrt{2} k_z T^{1-H}} \right)^{\frac{1}{H}} \quad [11]$$

Finally, we can evaluate  $N$  as the ratio between the resolution cell area  $A$  and the scatterer area  $\pi \tau_M^2$ :

$$N = \frac{A}{\pi \left( \frac{\sqrt{t}}{\sqrt{2} k_z T^{1-H}} \right)^{\frac{2}{H}}} \quad [12]$$

Therefore,  $N$  is a function of the surface fractal parameters, of the threshold  $t$ , of the resolution cell area, and of  $k_z = (2\pi / \lambda) * \cos\theta$ , i.e. of the signal wavelength and of the local incidence angle  $\theta$ . Without losing generality, in the following we always set  $t=1$ .

In Figure 2  $N$  is plotted as a function of  $T$  assuming the parameters of the Cosmo-SkyMed high resolution SAR sensor, i.e. a resolution cell area of 1 m<sup>2</sup>, a wavelength of 3.1 cm and a look angle of 30°. As shown by the graph the number of scatterers per resolution cell falls below 10 in many practical situations. Note that the range for  $T$  and  $H$  has been chosen in accordance to typical values of natural surfaces, as reported in the specialized literature [Brown and Scholz, 1985; Dierking, 1999; Di Martino et al., 2013].

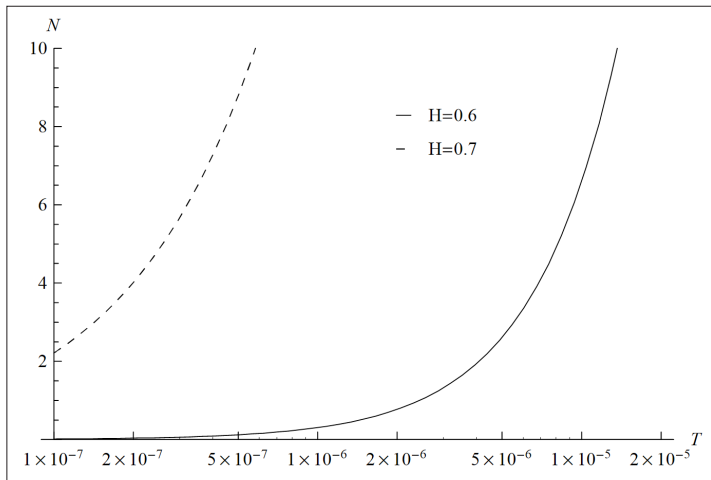


**Figure 2 - Plot of  $N$  as a function of  $T$  [m] assuming the Cosmo-SkyMed parameters reported in the text of the paper ( $T$ -axis is in logarithmic scale).**

## Simulation approach

The novel simulation approach proposed in this paper is based on the SARAS simulator [Franceschetti et al., 1992] and upgrades its capabilities to the simulation of non-fully developed speckle. As a matter of fact, while simulation of fully developed speckle can be performed without any supplementary information about the physical properties of the observed surface - supporting the wrong idea that the speckle is a simple multiplicative noise superimposed to the original “clean” signal -, simulation of non-Exponential speckle requires a detailed knowledge of the microscopic characteristics of the roughness within the resolution cell, thus unveiling the fact that speckle bears important information on otherwise inaccessible characteristics of the scene under survey. From this viewpoint, in this paper first results regarding the quantitative analysis of the effects of surface microscopic features on the behaviour of SAR images are presented: this is possible thanks to the joint use of the above described models and of reliable simulation techniques.

The focused SAR image can be expressed through relation [8], which makes clear that SAR simulation involves the evaluation of both the reflectivity function of the scene and the system unit response. In particular, the evaluation of the reflectivity function requires both a geometric and an electromagnetic characterization of the observed scene, while the SAR system unit response is a function of the radar data (RD) and orbital data (OD) of each specific sensor.

The proposed simulator is based on sound geometric and electromagnetic models [Franceschetti et al., 2002; Franceschetti and Riccio, 2007], effectively used for the evaluation of the reflectivity function of the scene. The transfer function of the system is evaluated and used for the generation of the SAR raw signal, which after standard processing provides the final image. The simulator requires as input the electromagnetic characterization of the scene, in terms of relative *dielectric constant*  $\epsilon$  and *conductivity*  $\sigma$  [S/m], RD and OD of the sensor of interest, a Digital Elevation Model (DEM) providing

the macroscopic - i.e., for spatial scales larger than the sensor resolution - description of the topography  $z(x,y)$ , and the description of the microscopic roughness within the resolution cell, in terms of the fractal parameters ( $H$  and  $T$ ) of the considered surface.

In this work we propose an update of the SARAS simulator, regarding the speckle synthesis. In the original version of the simulator speckle is synthesized assuming a fully developed Exponential intensity model. For each resolution cell the value of the complex reflectivity function - computed using direct electromagnetic models [Franceschetti and Riccio, 2007] - is multiplied by an appropriate complex circular Gaussian random variable, dictating an Exponential distribution for the image intensity. In the proposed updated simulator, as a preliminary step, the number of equivalent scatterers is obtained using [12]. The inputs needed for the evaluation of  $N$  are:

- the fractal parameters  $H$  and  $T$ , describing the microscopic roughness of the surface (i.e., the same used for the evaluation of  $\gamma$ );
- the wavelength  $\lambda$  and the resolution cell area  $A$ , which can be easily obtained from the RD block;
- the local incidence angle  $\vartheta$ , which can be obtained from the joint use of sensor look angle  $\theta_0$  (provided by the RD block) and DEM.

Then, the signal speckle component is evaluated according to [1], i.e. as the sum of the stochastic contributions due to the individual equivalent scatterers present within the resolution cell, where the amplitudes  $V_i$  of these contributions are distributed according to [2], while the phases  $\varphi_i$  are uniformly distributed in  $(0,2\pi)$ .

As a first step, we generate K-distributed pseudo-random numbers presenting the pdf in [2] using a 2-D Gaussian scale mixture model expressed as [Eltoft, 2006]:

$$\mathbf{Y} = \sqrt{Z} \mathbf{X} \quad [13]$$

where  $\mathbf{X}$  is a two-dimensional zero-mean Gaussian variable with covariance matrix equal to the identity matrix and  $Z$  is a scalar  $\Gamma$ -distributed random variable independent from  $\mathbf{X}$ . With these assumptions the modulus of  $\mathbf{Y}$  will held the distribution in [2], whose parameters are related to those of the  $\Gamma$  distribution considered for  $Z$  [Eltoft, 2006]. In particular, the scale and shape parameters of  $Z$  are equal to  $b^2/2$  and  $\nu$ , respectively. Then, summing up coherently the obtained values for each scatterer over the total number of equivalent scatterers  $N$  we get the distribution [3]. Finally, we multiply the obtained value of the speckle component by the mean square value of the backscattered field. However, as a preliminary step, we must impose that the distribution in [3] holds a unitary mean in order to preserve the mean square value of the backscattered field. This is obtained fixing the value of  $b$  - according to the relation in [5] - to

$$b = 2\sqrt{M} \quad [14]$$

In Figure 3 a block scheme of the proposed simulator is shown, where  $h(x,r)$  is the raw signal and  $r$  stands for the slant range coordinate. In the following section relevant simulation results are presented and analysed.

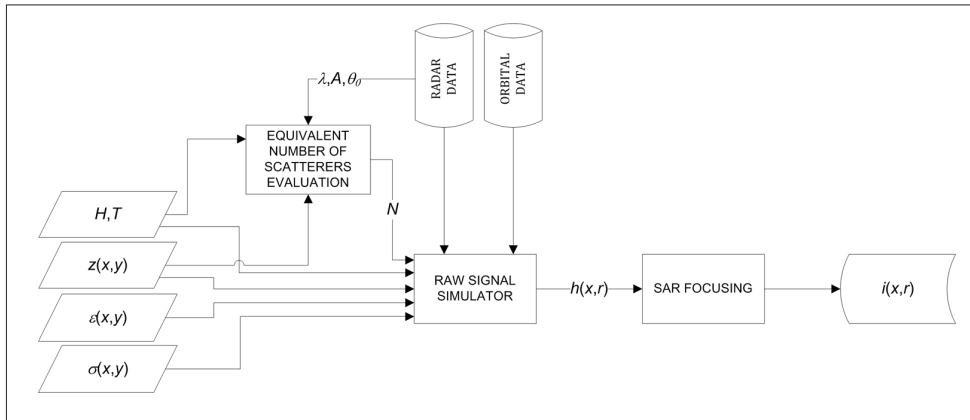


Figure 3 - Block scheme of the simulator.

## Results

In the following we report the first results regarding the simulation of rather simple canonical scenes, in order to present a validation of the proposed simulation approach. In particular, we implemented the simulation chain described in the previous section and simulated four SAR images relevant to a flat surface with constant electromagnetic parameters in order to obtain a homogeneous scene. On the four images the number of equivalent scatterers per resolution cell  $N$  is assumed to be 1, 2, 5, while in the last case fully developed speckle is generated, using the algorithm already available in the SARAS simulator [Franceschetti et al., 1992]. Note that the simulator requires as input also the value of  $\nu$ . An indication of the possible range of values for this parameter is found in [Jakeman and Pusey, 1976] and references therein, where it is suggested to consider  $-0.7 \leq \nu \leq 3$ . Further research is necessary to better understand how to determine this parameter for actual data. However, in all the simulated scenarios presented in this work  $\nu$  is set equal to 1. We explicitly note that for the simulations reported here the knowledge of the specific parameters determining the value of  $N$  is of no practical interest: the statistics for a homogeneous scene are dictated only by  $N$ , no matter what values of fractal parameters and RD data were used to obtain it. In Figure 4 patches of  $256 \times 256$  pixels cropped from the simulated intensity images are shown. As a matter of fact, it is very hard to draw significant conclusions only on the basis of visual inspection of the presented images. For this reason, in Figure 5 the pdf relevant to the images are presented. It is evident that the behaviour of the graphs tends to converge very quickly to the Exponential distribution, i.e. to the distribution expected in case of fully developed speckle. We note that the results presented in Figure 5 experience an underestimation of the occurrence of low intensity values with respect to the theoretical ones shown in Figure 1. Anyway, the behaviour of the pdf as a function of  $N$  is in agreement with the theoretical one.

Looking at the pdf in Figure 5 it is not easy to discriminate between the behaviours of the different distributions, especially when the number of scatterers increases. For this reason, in Figure 6 we provide the graphs (in semi-logarithmic scale) of the first nine normalized intensity moments estimated from the images in Figure 4 (in black) compared with the

theoretical ones (in red). As a matter of fact, the normalized moments are able to better highlight the differences in the distribution shapes. The expression of the normalized moments of the K distribution [4] taking into account the assumption [14] becomes:

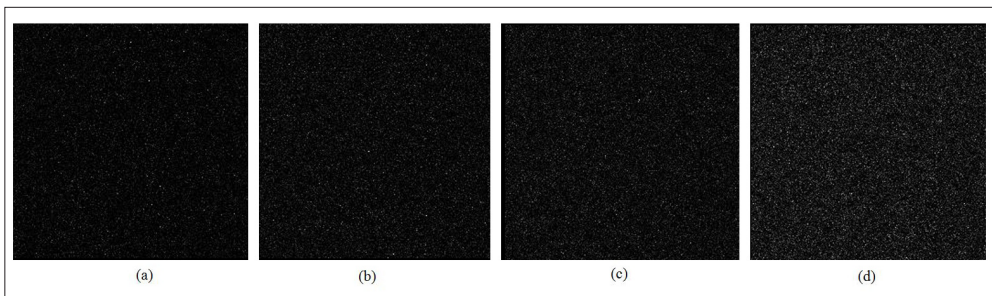
$$\frac{\langle w^n \rangle}{\langle w \rangle^n} = \frac{n! \Gamma(n+M)}{M^n \Gamma(M)} \quad [15]$$

Looking at Figure 6 an easier discrimination of the different distributions can be attained. Moreover, a good agreement between the simulated and theoretical cases can be appreciated, especially for lower order moments. In fact, the estimation of higher order moments is expected to be less accurate, the sample sizes being equal [Joughin et al., 1993]. Finally, we note that the most widespread techniques for the estimation of the K distribution parameters from measured data are based on the estimation of the second order moment [Jakeman and Pusey, 1976; Joughin et al., 1993]. Along this guideline we estimated the value of  $N$  from the simulated images reported in Figure 4. The obtained results are presented in Table 1.

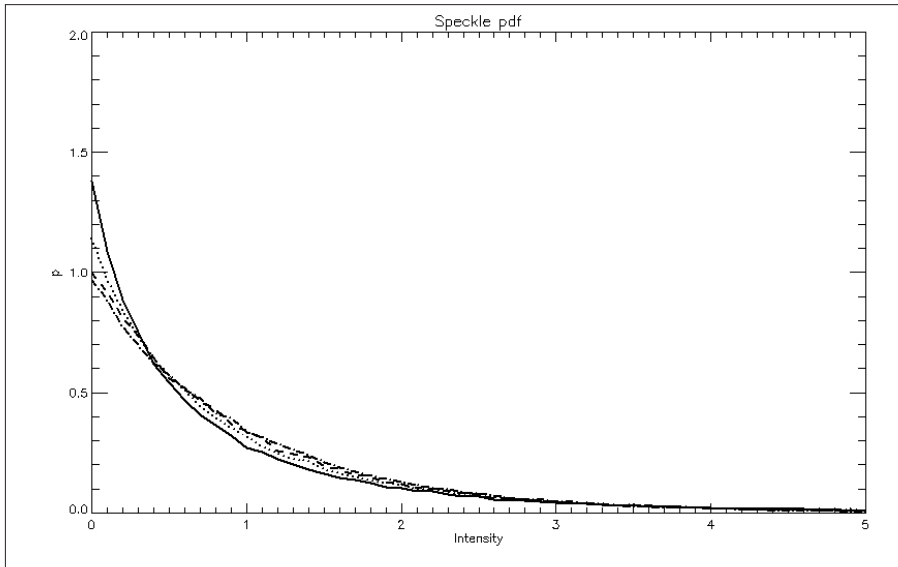
**Table 1 - Estimation Results.**

Figure	Estimated $N$	Expected $N$
4 (a)	1.3	1
4 (b)	2.8	2
4 (c)	6.4	5
4 (d)	163	$\infty$

It can be noted that the estimates suffer of overestimation, which probably can be related to the introduction of some degree of correlation in the data due to the sensor impulse response. However, apart from this effect, the obtained estimates allow an easy detection of the variations of  $N$  between the different cases.



**Figure 4 - Simulated SAR images: (a)  $N=1$ , (b)  $N=2$ , (c)  $N=5$ , (d) Exponential ( $N=\infty$ ).**



**Figure 5 - Pdf of the simulated images:  $N=1$  (full line),  $N=2$  (dotted line),  $N=5$  (dashed line), Exponential (dash-dotted line).**

## Conclusions

In this paper a framework for the simulation of SAR images with K-distributed speckle statistics is introduced. The proposed simulation framework allows quantitative studies of the physical information (on the observed surface) held by the speckle component. In fact, the proposed approach is based on the knowledge of the number of scatterers per resolution cell, which for fBm surfaces has been analytically evaluated by the authors in a recent work. Therefore, the proposed method decisively departs from those based only on a statistical noise-like characterization of the speckle phenomenon, quantitatively assessing its relation with surface relevant physical parameters.

The synthesis of the speckle statistics is effectively accomplished through the introduction of a 2-D scale mixture of Gaussian variables in a SAR raw signal simulator previously developed by some of the authors. In the final section, the presented preliminary results highlight the potentialities of the proposed simulator, through the analysis of the statistical behaviour of a small set of simulated images and a comparison with results relevant to the fully developed speckle case. Also some meaningful inversion results, regarding the estimation of  $N$  from simulated data are reported.

In this paper first result of the analysis of rather simple simulation conditions are presented, and further investigations will be necessary in order to better understand the influence of significant scene and sensor parameters on the overall statistical behaviour of the simulated images. This kind of study is a prerequisite for the development of techniques allowing the inversion of the proposed physical models. From this viewpoint, also the extension of the simulation technique to non-integer values of  $N$  will be an important step in order to investigate a wider range of practical situations (e. g., the case of sea surfaces).

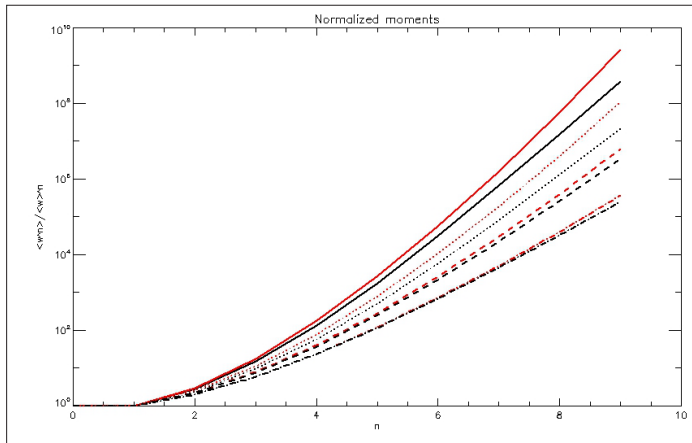


**Figure 6 - Normalized moments of the simulated images (in black) compared to the theoretical ones (in red):  $N=1$  (full line),  $N=2$  (dotted line),  $N=5$  (dashed line), Exponential (dash-dot line).**

## Acknowledgements

This work has been supported by the EU-FP7 project “Development of Pre-Operational Services for Highly Innovative Maritime Surveillance Capabilities” (DOLPHIN).

## References

- Beckman P., Spizzichino A. (1963) - *The Scattering of Electromagnetic Waves from Rough Surfaces*. New York: Pergamon Press.
- Brown S.R., Scholz C.H. (1985) - *Broad-band study of the topography of natural rock surfaces*. Journal of Geophysical Research, 90 (B14): 12575-12582. doi: <http://dx.doi.org/10.1029/JB090iB14p12575>.
- Collins M.J., Allan J.M. (2009) - *Modeling and Simulation of SAR Image Texture*. IEEE Transactions on Geoscience and Remote Sensing, 47 (10): 3530-3546. doi: <http://dx.doi.org/10.1109/TGRS.2009.2021260>.
- Dierking W. (1999) - *Quantitative Roughness Characterization of Geological Surfaces and Implications for Radar Signature Analysis*. IEEE Transactions on Geoscience and Remote Sensing, 37 (5): 2397-2412. doi: <http://dx.doi.org/10.1109/36.789638>.
- Di Martino G., Iodice A., Riccio D., Ruello G. (2007) - *A Novel Approach for Disaster Monitoring: Fractal Models and Tools*. IEEE Transactions on Geoscience and Remote Sensing, 45 (6): 1559-1570. doi: <http://dx.doi.org/10.1109/TGRS.2006.887024>.
- Di Martino G., Iodice A., Riccio D., Ruello G. (2010) - *Physical-based models of speckle for high resolution SAR images*. Proceedings of the IEEE International Geoscience and Remote Sensing Symposium 2010: 2980-2983. doi: <http://dx.doi.org/10.1109/IGARSS.2010.5649378>.
- Di Martino G., Iodice A., Riccio D., Ruello G. (2012) - *Electromagnetic characterization of speckle in SAR images*. Atti della Riunione Nazionale di Elettromagnetismo 2012: 613-616.
- Di Martino G., Poderico M., Poggi G., Riccio D., Verdoliva L. (2012a) - *SAR image simulation for the assessment of despeckling techniques*. Proceedings of the IEEE

- International Geoscience and Remote Sensing Symposium 2012: 1797-1800. doi: <http://dx.doi.org/10.1109/IGARSS.2012.6351163>.
- Di Martino G., Iodice A., Riccio D., Ruello G. (2013) - *Equivalent Number of Scatterers for SAR Speckle Modeling*. IEEE Transactions on Geoscience and Remote Sensing, in press. doi: <http://dx.doi.org/10.1109/TGRS.2013.2262770>.
- Di Martino G., Poderico M., Poggi G., Riccio D., Verdoliva L. (2013a) - *Benchmarking Framework for SAR Despeckling*. IEEE Transactions on Geoscience and Remote Sensing, in press. doi: <http://dx.doi.org/10.1109/TGRS.2013.2252907>.
- Eltoft T. (2006) - *A new approach to modeling signal amplitude statistics by the K distributions*. Proceedings of the 7th Nordic Signal Processing Symposium 2006: 62-65. doi: <http://dx.doi.org/10.1109/NORSIG.2006.275277>.
- Falconer K. (1989) - *Fractal Geometry*. Chichester, U.K., Wiley.
- Feder J.S. (1988) - *Fractals*. New York: Plenum. doi: <http://dx.doi.org/10.1007/978-1-4899-2124-6>.
- Franceschetti G., Migliaccio M., Riccio D., Schirinzi G. (1992) - *SARAS: a Synthetic Aperture Radar (SAR) raw signal simulator*. IEEE Transactions on Geoscience and Remote Sensing, 30 (1): 110-123. doi: <http://dx.doi.org/10.1109/36.124221>.
- Franceschetti G., Migliaccio M., Riccio D. (1994) - *SAR raw signal simulation of actual ground sites described in terms of sparse input data*. IEEE Transactions on Geoscience and Remote Sensing, 32 (6): 1160-1169. doi: <http://dx.doi.org/10.1109/36.338364>.
- Franceschetti G., Riccio D. (2007) - *Scattering, Natural Surfaces and Fractals*. Burlington, MA: Academic.
- Goodman J.W. (1976) - *Some fundamental properties of speckle*. Journal of the Optical Society of America, 66 (11): 806-814. doi: <http://dx.doi.org/10.1364/JOSA.66.001145>.
- Goodman J.W. (2008) - *Speckle with a finite number of steps*. Applied Optics, 47 (4): 111-118. doi: <http://dx.doi.org/10.1364/AO.47.00A111>.
- Jakeman E., Pusey P.N. (1976) - *A Model for Non-Rayleigh Sea Echo*. IEEE Transactions on Antennas and Propagation, 24 (6): 1145-1150. doi: <http://dx.doi.org/10.1109/TAP.1976.1141451>.
- Jakeman E., Pusey P.N. (1978) - *Significance of K distribution in scattering experiments*. Physical Review Letters, 40 (9): 546-550. doi: [0.1103/PhysRevLett.40.546](http://dx.doi.org/10.1103/PhysRevLett.40.546).
- Joughin I.R., Percival D.B., Winebrenner D.P. (1993) - *Maximum Likelihood Estimation of K Distribution Parameters for SAR Data*. IEEE Transactions on Geoscience and Remote Sensing, 31 (5): 989-999. doi: <http://dx.doi.org/10.1109/36.263769>.
- Lee J.S., Jurkevich I. (1989) - *Segmentation of SAR images*. IEEE Transactions on Geoscience and Remote Sensing, 27 (6): 674-680. doi: <http://dx.doi.org/10.1109/36.35954>.
- Mandelbrot B. B. (1983) - *The Fractal Geometry of Nature*. New York, Freeman.
- Oliver C.J. (1984) - *A model for non-Rayleigh scattering statistics*. Optica Acta, 31 (6): 701-722. doi: <http://dx.doi.org/10.1080/713821561>.
- Raney R.K., Wessels G.J. (1988) - *Spatial considerations in SAR speckle simulation*. IEEE Transactions on Geoscience and Remote Sensing, 26 (5): 666-672. doi: <http://dx.doi.org/10.1109/36.7693>.
- Shepard M.K., Campbell B.A., Bulmer M.H., Farr T.G., Gaddis L.R., Plaut J.J. (2001) - *The roughness of natural terrain: A planetary and remote sensing perspective*. Journal of Geophysical Research, 106 (E12): 32777-32795. doi: <http://dx.doi.org/10.1029/>

2000JE001429.

- Tello M., Bonastre R., Lopez-Martinez C., Mallorqui J.J., Danisi A., Di Martino G., Iodice A., Ruello G., Riccio D. (2007) - *Characterization of local regularity in SAR imagery by means of multiscale techniques: application to oil spill detection*. Proceedings of the IEEE International Geoscience and Remote Sensing Symposium 2007: 5228-5231. doi: <http://dx.doi.org/10.1109/IGARSS.2007.4424040>.
- Tomiyasu K. (1983) - *Computer Simulation of Speckle in a Synthetic Aperture Radar Image Pixel*. IEEE Transactions on Geoscience and Remote Sensing, GE-21 (3): 357-363. doi: <http://dx.doi.org/10.1109/TGRS.1983.350566>.
- Watts S., Baker C. J., Ward K. D. (1990) - *Maritime surveillance radar Part 2: Detection performance prediction in sea clutter*. IEE Proceedings F, Radar and Signal Processing, 137 (2): 63-72. doi: <http://dx.doi.org/10.1049/ip-f-2.1990.0010>.